49th IEEE Conference on Decision and Control
December 15-17, 2010
Hilton Atlanta Hotel, Atlanta, GA, USA

Real-time synchronization feedbacks for single-atom frequency standards: V- and Λ-structure systems

Mazyar Mirrahimi, Alain Sarlette and Pierre Rouchon

Abstract— **This paper proposes simple feedback loops, inspired from extremum-seeking, that use the photon emission times of a single quantum system following quantum Monte-Carlo trajectories in order to lock in real time a probe frequency to the system's transition frequency. Two specific settings are addressed: a 3-level system coupling one ground to two excited states (one highly unstable and one metastable) and a 3-level system coupling one excited to two ground states (both metastable). Analytical proofs and simulations show the accurate and robust convergence of probe frequency to system-transition frequency in the two cases.**

I. INTRODUCTION

The SI second is defined to be "the duration of 9 192 631 770 periods of the radiation corresponding to the transition between the two hyperfine levels of the ground state of the caesium 133 atom" [1]. A primary frequency standard is a device that realizes this definition. For micro atomic-clocks [8] perfect resonance between the probe laser frequency and the atomic frequency is characterized by a maximum (or minimum) output signal of a photo-detector. Therefore extremum seeking techniques (see e.g [3] for a recent exposure) are usually used in high precision spectroscopy to achieve frequency lock with an atomic transition frequency [14], [12], [13].

State-of-the-art experiments appear in two strategies. In a first strategy A, a real-time synchronization feedback scheme based on modulation of the probe frequency (see more description in [9]) is applied to a large population of identical quantum systems with few mutual interactions (the vapor cell) having reached its asymptotic statistical regime; the evolution of this population and the related output signal follow the continuous density matrix dynamics of a static Lindblad-Kossakovski master equation. In a second strategy B (see e.g. [13], [11]), a single atom is probed for a long time with different probe frequencies and locking with the atom transition frequency is deduced from the resulting statistics; this somehow reconstructs over time the continuous signal corresponding to strategy A.

The present paper proposes a way to merge the two strategies and adapt real-time synchronization feedback to a single quantum system. Such a single system cannot be described by a static non-linear input/output map but it obeys stochastic jump dynamics [5], [7], modeled by "quantum Monte-Carlo" trajectories; with respect to strategy A, the output signal is no more continuous but corresponds to a counter giving the jump times. As shown in [4], all the spectroscopic information and in particular the value of the atomic transition frequency are contained in the statistics of these jump-time series. The novelty of the present paper is to avoid the use of quantum filters [6] and records of jump-time sequences required by usual statistical treatments as in strategy B. It proposes a real-time synchronization feedback scheme that can be implemented on electronic circuits of similarly low complexity as those used for extremum-seeking loops in strategy A. The resulting real-time synchronization scheme might also allow to track (e.g. field-induced) variations in the atom's transition frequency with a reasonable bandwidth, depending on the particular atomic clock system.

We consider two particular atomic systems in the present paper. **(1)** The first one corresponds to a V-system, which features the electron-shelving mechanism and is one of the main candidates for atomic clocks [4]. The system has two excited states — one unstable and one metastable — which interact with the same ground state through two electromagnetic fields. The system mostly evolves through the ground-to-unstable transition. However, accurate frequency estimation is based on the ground-to-metastable transition. **(2)** The second setting corresponds to a Λ-system, where two electromagnetic fields are tuned to make two metastable ground states both interact with the same unstable excited state. This system typically appears in coherent population trapping phenomena and optical pumping [2], but also in micro atomic clocks. This second setting is studied in more detail in [9].

For the two systems, we propose relevant forms of the amplitude modulation of the probe electromagnetic fields and the associated real-time updates for their frequency on the basis of photon detection times. We establish the stochastic convergence property of probe frequency towards atomic transition frequencies.

Note that the "quantum Monte-Carlo" trajectories, used throughout the paper, should be understood as the actual model for a single quantum system's behavior, and not as a numerical method. We refer to [7] for more details on the physical interpretation of these quantum dynamics.

The paper is organized as follows. Sections II and III consider, respectively, the V-system and the Λ-system.

This paper is part of the SIAM session; it summarizes and extends the work described in [9]. M.Mirrahimi is with the INRIA research center, Rocquencourt, France. A.Sarlette is an FNRS postdoctoral researcher (Belgian National Research Fund), currently visiting at Mines ParisTech. P.Rouchon is professor at Mines ParisTech, Centre Automatique et Systèmes. mazyar.mirrahimi@inria.fr, alain.sarlette@ulg.ac.be, pierre.rouchon@mines-paristech.fr

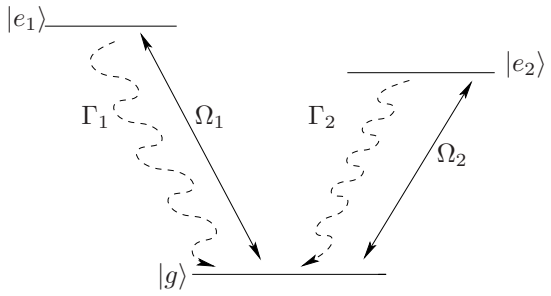

Fig. 1. The V structure system: a ground state $|g\rangle$ is coupled by two electromagnetic fields to a highly unstable state $|e_1\rangle$ ("blue laser") and a metastable state $|e_2\rangle$ ("red laser").

Each section first describes main properties of the specific stochastic dynamics, then proposes a synchronization feedback with the main ideas of a convergence proof, and finally presents simulation results along with comments on the performance. For detailed proofs the reader is referred a.o. to [9].

II. THE V-SYSTEM

A. System dynamics and reduction

The V-system evolves on the Hilbert space spanned by a stable ground state $|g\rangle$, an unstable excited state $|e_1\rangle$, and a metastable excited state $|e_2\rangle$ (see Fig. 1). Lifetimes of the excited states w.r.t. decaying to $|g\rangle$ are $1/\Gamma_1$ and $1/\Gamma_2$, with $\Gamma_1 \gg \Gamma_2$ (see simulation section for typical values). The system is submitted to two laser fields with slowly varying amplitudes denoted by Ω_1, Ω_2, and frequencies near-resonant respectively with the $|g\rangle \leftrightarrow |e_1\rangle$ ("blue laser") and $|g\rangle \leftrightarrow |e_2\rangle$ ("red laser") transitions; the corresponding detunings are noted Δ_1 and Δ_2. The goal is to reach $\Delta_2 = 0$, i.e. to exactly synchronize the red laser to the transition frequency $\frac{E_{e2}-E_g}{\hbar}$. Indeed, thanks to the large lifetime of metastable state $|e_2\rangle$, the uncertainty on this energy difference is very narrow.

The classical rotating wave approximation, which assumes frequencies associated to transition energies $\frac{E_{e1}-E_g}{\hbar}$, $\frac{E_{e2}-E_g}{\hbar}$, $\frac{E_{e1}-E_{e2}}{\hbar}$ to be much larger than all other characteristic frequencies, yields the following quantum Markov trajectory model for the density matrix ρ characterizing a single system (where $\{a,b\} = ab + ba$):

- continuous-time (1)

$$\frac{d}{dt}\rho = -\imath[\tfrac{H}{\hbar},\rho] - \tfrac{1}{2}\sum_{j=1}^{2}\left\{Q_j^\dagger Q_j,\rho\right\} + \sum_{j=1}^{2}\mathrm{trace}(Q_j^\dagger Q_j\rho)\rho$$

$$\text{with } \tfrac{H}{\hbar} = \Delta_1|e_1\rangle\langle e_1| + \Delta_2|e_2\rangle\langle e_2| + \textstyle\sum_{j=1}^{2}\frac{\Omega_j Q_j^\dagger + \Omega_j^* Q_j}{\sqrt{\Gamma_j}}$$

$$Q_1 = \sqrt{\Gamma_1}|g\rangle\langle e_1| \qquad \text{and} \qquad Q_2 = \sqrt{\Gamma_2}|g\rangle\langle e_2|$$

- jump to $\rho = |g\rangle\langle g|$ during dt with probability

$$P_{\text{jump}}(\rho \to |g\rangle\langle g|) = \textstyle\sum_{j=1}^{2}\mathrm{trace}(Q_j^\dagger Q_j\rho)dt = \sum_{j=1}^{2}\Gamma_j\langle e_j|\rho|e_j\rangle dt\ .$$

Assuming that decoherence rate Γ_1 (typically $10^9\,Hz$) is much larger than all other characteristic frequencies, singular perturbation and center manifold theories are applied as explained in [10] to separate slow and fast dynamics[1]. The resulting dynamics describe a two-level "slow" system essentially on the $|g\rangle \leftrightarrow |e_2\rangle$ transition. It can be written on the Bloch sphere (see e.g. textbook [7]) as follows, with $Z = -1$ and $Z = +1$ corresponding to $|g\rangle$ and $|e_2\rangle$ respectively.

- $\begin{aligned} \tfrac{d}{dt}X &= vZ + \Delta_2 Y + \tfrac{\sigma}{2}(-Z\,X) \\ \tfrac{d}{dt}Y &= -uZ - \Delta_2 X + \tfrac{\sigma}{2}(-Z\,Y) \\ \tfrac{d}{dt}Z &= -vX + uY + \tfrac{\sigma}{2}(1-Z)(1+Z) \end{aligned}$ (2)
- and jump to $Z = -1$ with probability

$$P_{\text{jump}}(Z \to -1) = \left(\Gamma_2 + \tfrac{\sigma}{2}\,(1-Z)\right)dt \qquad (3)$$

We denote $\Omega_2 = u + \imath\, v$ and $\sigma = (\frac{\Omega_1^2}{\Gamma_1} - \Gamma_2)$. Since $\Gamma_2 \ll$, it is reasonable that $\frac{\Omega_1^2}{\Gamma_1} \gg \Gamma_2$ such that $\sigma > 0$.

Observations:

1. Fortunately Δ_1 does not appear in these dynamics.
2. In absence of photon emission jumps, the decoherence term, proportional to σ, drives the system towards *excited* state $|e_2\rangle$, not towards $|g\rangle$ as is usually the case for a two-level system. This reflects the effect of measurement with the blue laser: if no photon is emitted despite a strong coupling of $|g\rangle$ with $|e_1\rangle$, then it is most probable that the system is actually mainly "shelved" on state $|e_2\rangle$. Of course the system still jumps to $|g\rangle$ at photon emission.

B. Synchronization feedback

In the absence of jumps, (2) is strictly equivalent to the two-level system of [9], after inversion of the Z-direction (and controls u, v) and scaling by $\frac{\sigma}{\Gamma_1}$. Therefore we take

$$\Omega_2 = \bar{u}(1 + \imath\cos(\omega t)) \qquad (4)$$

as for this two-level system, with $\bar{u} = 2\kappa\sigma\epsilon$ w.r.t. the proof in [9]. Jump dynamics (3) after Z-inversion features a significant difference w.r.t. the two-level system of [9]: the system jumps to the *opposite point* of the Bloch sphere at photon emission. The jumping *probability* after Z-inversion is however as in [9]. Therefore, the analogous update is:

$$\begin{cases} \Delta_2(N+1) = \Delta_2(N) + \delta\,\bar{u}\,\sin(\omega\,t_N) \\ \qquad\qquad \text{if} \quad |\Delta_2(N) + \delta\,\bar{u}\,\sin(\omega\,t_N)| \le C, \\ \Delta_2(N+1) = C \qquad \text{otherwise} \end{cases} \qquad (5)$$

where t_0, t_1,... t_N,... are the detection times of photons *that are preceded by a sufficiently long "dead-time" interval* $[t_N - T,\, t_N)$ during which no photon has been detected, for some $T > 0$. Thus (5) is only applied for photons that follow a sufficiently long evolution without jump. While a similar condition is included in [9] as a technicality, here T plays

[1]This is done by using the corresponding deterministic *ensemble* dynamics, in Lindblad-Kossakovski master equation form, as an intermediate step. See details for a similar case in Section III.

a crucial role, explained in the following. We assume as in [9] that initially $|\Delta|$ does not exceed a fixed constant C and explicitly maintain it within this bound.

The idea behind (4), similarly for the two-level system in [9], is: under (4),(2) the system ultimately converges to and evolves on a limit cycle in the neighborhood of $Z = 1$. The position of this limit cycle, and linked to this the phase of the system on the limit cycle w.r.t. the phase in (4), depends on Δ_2. The jump probability will depend on the position on the limit cycle, and thus jump times reflect Δ_2.

Under (4), the system in absence of jumps slowly drifts from $|g\rangle$ towards $|e_2\rangle$, around which it stabilizes on a limit cycle; when jumping, the system goes to $|g\rangle$; the jump probability *decreases* when going from $|g\rangle$ to $|e_2\rangle$. As a consequence the system jumps to a point (i) that is opposite to the limit cycle on which we want to use (5) and (ii) in whose neighborhood jumping again is highly probable. Therefore, a useful photon for (5), based on limit-cycle evolution as explained in the previous paragraph, is gained only rarely, when the system travels the whole way from one pole of the sphere to the other without emitting a photon. Physically, (5) is applied close to an electron-shelving state, which is much less probable to reach than emitting many photons on the $|g\rangle \leftrightarrow |e\rangle$ transition.

Consequently, we must impose a "dead-time" T large enough to ensure that the system has travelled the whole way from $|g\rangle$ to the limit cycle around $|e_2\rangle$; in contrast, for the systems studied in [9] (see also Section III), T is introduced essentially as a technicality. However, the longer time invested is compensated by better accuracy: the scaling w.r.t. two-level system of [9], due to the long lifetime of $|e_2\rangle$, implies that (2) is sensitive to $\frac{\Gamma_1}{\sigma}$ times smaller Δ_2. It also requires $\frac{\Gamma_1}{\sigma}$ times smaller ω. Note that the dead-time detection can be replaced by detection of a "*red* photon" if a narrow-band detector is available in the experiment.

Theorem 1: Consider the Monte-Carlo trajectories described by (2),(3) with controller (4),(5). Assume $\sigma = (\frac{\Omega_1^2}{\Gamma_1} - \Gamma_2) > 0$ and take $\bar{u} \sim \sigma\,\epsilon,\ \delta \sim \sigma\,\epsilon^2$ with $\epsilon \ll 1$. For initial detuning C, assume $4C^2 + 1 < 4\omega^2$. Then there exists a dead-time T large enough so that

$$\limsup_{N\to\infty} \mathbb{E}(\Delta_2(N)^2) \leq O(\epsilon^2)\,.$$

Indeed, thanks to the analogy between our reduced system and the two-level system of [9], conclusions of Theorem 2.1 and Corollary 2.2 in [9] can be transposed here *assuming the system reduction to be exact*. For the original system, we need Γ_1 so large that (1),(4) has a limit cycle ϵ^4-close to the one estimated with the reduced system in the proof, see [9].

C. Simulation and discussion

The simulation is made on the full model (1). Parameters are chosen as $\Gamma_1 = 5$, $\Omega_1 = 0.5$, $\Delta_1 = 0$, $\Gamma_2 = 0.005$, $\bar{u} = 0.04$, $\omega = 0.08 \cdot 2\pi$, $\delta = 0.012$ and $T = 100$. With these values, about 1 out of 100 photons corresponds to a jump after sufficient dead-time, thus an update. Figure 2 shows the evolution of detuning for a single trajectory of the system. During the overall time of $24 \cdot 10^5$ the detuning decreases from 0.25 to 0.03. As suspected given the significant dead-time, convergence is much slower than for the systems described in [9], see also Section III. For a typical system with Γ_1 in the nano-second range, the full simulation time is of the order of $1ms$ and the obtained accuracy is about $\frac{\Gamma_1}{100} \sim 10\,MHz$.

Figure 3 shows a typical section of quantum Monte-Carlo trajectory for the same simulation. It represents $\langle e_2|\rho|e_2\rangle$, that is the probability of being "shelved" on metastable state $|e_2\rangle$. Each jump down to 0 corresponds to the emission of a photon. Each plateau close to 1 corresponds to a "shelved electron" situation. There is a significant probability to emit no photon for a long time on this plateau, which has led to its name "dark window" in the physics literature [4]. Oscillations on the plateau due to periodic excitation (4) are clearly visible. Jumping from the plateau corresponds to a "red" photon and triggers a detuning update. The idea behind (5) is that jumps are more probable in the "valleys" of the oscillations.

Simulations and approximate reasoning confirm that small laser amplitudes Ω_1, Ω_2 improve the synchronization accuracy. Note that in addition to Theorem 1, accuracy of the singular perturbation approximation must be taken into account. In practice, synchronization accuracy is limited by the following.

- For small Ω_1, Ω_2, it takes longer to travel from $|g\rangle$ to the neighborhood of $|e_2\rangle$ where useful information is gained. Thus convergence becomes very slow.
- Requirement $\sigma > 0$ imposes $\Omega_1^2 > \Gamma_2\,\Gamma_1$ where the right side is a system property. This lower bound on Ω_1 sets a limit for the accuracy of the singular perturbation approximation. Thus unlike for the two-level system, it is not possible here[2] to reach arbitrary accuracy by taking small controls.
- One advantage of the V-system for physical experiments is that the blue laser is also used for cooling atomic motion [15]. This Doppler cooling technique requires significant amplitude Ω_1 and detuning Δ_1: optimum cooling is achieved at $\Omega_1 = \Gamma_1$ and $\Delta_1 = -\frac{\Gamma_1}{2}$. With these choices the singular perturbation approximation clearly fails. A proper reduction of fast vs. slow dynamics would then reduce the slow "system" to the one-dimensional $|e_2\rangle$-space: the system varies in first approximation between two discrete situations, either completely trapped on $|e_2\rangle$, or constantly moving between $|g\rangle$ and $|e_1\rangle$ with rapid photon emission. Then real-time synchronization feedback schemes analogous to the ones in this paper cannot be proposed anymore.

Sensitivity of the system to Ω_1 and Δ_1 is known by physicists as "ground state broadening and shifting" through the laser-induced interaction of $|g\rangle$ with $|e_1\rangle$. This effect can

[2]That is, on the *original* V-system (1), in contrast to singular perturbation approximation (2).

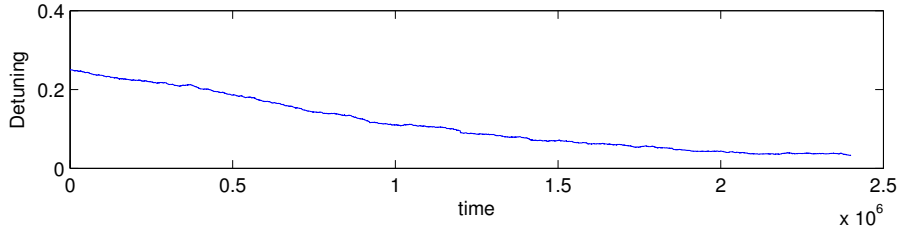

Fig. 2. Simulation of synchronization feedback on the V-system: evolution of detuning for a single Monte-Carlo trajectory.

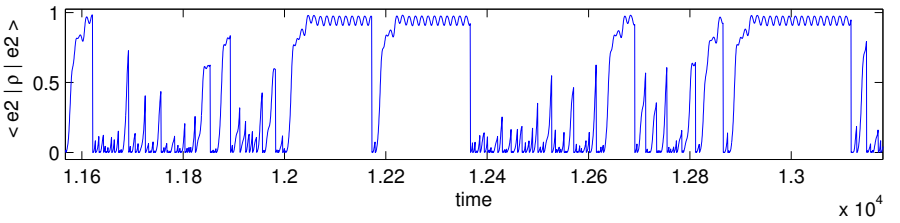

Fig. 3. Simulation of synchronization feedback on the V-system: quantum Monte-Carlo trajectory of $\langle e_2|\rho|e_2\rangle$.

be avoided in high-precision frequency measurements by turning on the blue and red lasers *alternatively*, as suggested in [4]. However, the real-time synchronization feedback proposed here does not work with dynamics modified in this way.

In conclusion, the proposed real-time feedback synchronization on the V-system seems not competitive for ultra-high-precision atomic clock standards like [11]. However, the real-time operation obtained in return (e.g. convergence in $1\,ms$ in the above simulation) might allow large-bandwidth tracking of *energy level variations* e.g. to track a physical parameter (magnetic field) on which $\frac{E_{e2}-E_g}{\hbar}$ depends.

III. THE Λ-SYSTEM

A. System dynamics and reduction

In this section, we consider a 3-level system in Λ-configuration, as another candidate for a frequency standard. The system is composed of two metastable ground states $|g_1\rangle$ and $|g_2\rangle$, and an excited state $|e\rangle$ coupled to the lower ones. The decay times for the $|e\rangle \to |g_j\rangle$ transitions are assumed to be much shorter than those corresponding to the transition between ground states (here assumed so lowly probable that it is neglected). Similarly to the previous section, we denote the associated relaxing constants by Γ_1 and Γ_2. However, we do not have anymore $\Gamma_2 \ll \Gamma_1$: our essential assumption is that both Γ_1 and Γ_2 are large w.r.t. other parameters. The ground states can have their energy separation in microwave regime, like in atomic microclocks, but also in the optical regime which would allow a better precision of the clock.

Once again, we consider near-resonant laser fields with slowly varying amplitudes that we note by $\widetilde{\Omega}_1$ and $\widetilde{\Omega}_2$ and the associated detunings Δ_e and $\Delta_e + \Delta$ (Δ is called the Raman detuning). Here we explicitly detail the derivation of the quantum Markov model describing single system trajectories, from the Lindblad master equation governing average dynamics of an ensemble of systems. The classical rotating wave approximation yields the following master equation of Lindblad type

$$\frac{d}{dt}\rho = -\frac{\imath}{\hbar}[\tilde{H},\rho] + \frac{1}{2}\sum_{j=1}^{2}(2Q_j\rho Q_j^\dagger - Q_j^\dagger Q_j\rho - \rho Q_j^\dagger Q_j), \quad (6)$$

with

$$\begin{aligned}\tfrac{\tilde{H}}{\hbar} =& \tfrac{\Delta}{2}(|g_2\rangle\langle g_2| - |g_1\rangle\langle g_1|)\\ &+ \left(\Delta_e + \tfrac{\Delta}{2}\right)(|g_1\rangle\langle g_1| + |g_2\rangle\langle g_2|)\\ &+ \widetilde{\Omega}_1|g_1\rangle\langle e| + \widetilde{\Omega}_1^*|e\rangle\langle g_1| + \widetilde{\Omega}_2|g_2\rangle\langle e| + \widetilde{\Omega}_2^*|e\rangle\langle g_2|\end{aligned}$$

and $Q_j = \sqrt{\Gamma_j}\,|g_j\rangle\langle e|$.

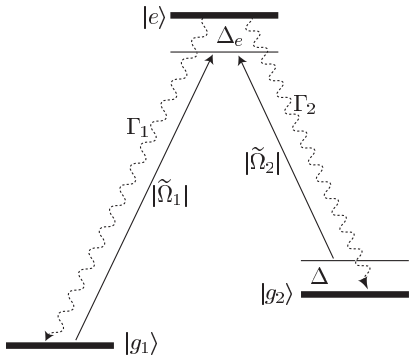

Fig. 4. The Λ-system: two metastable ground states $|g_1\rangle$ and $|g_2\rangle$ are coupled to an unstable excited state.

Assuming that the decoherence rates Γ_1 and Γ_2 are much larger than the Rabi frequencies $|\widetilde{\Omega}_1|$, $|\widetilde{\Omega}_2|$ and the detuning frequencies Δ and Δ_e, the system spends very little time on the excited state $|e\rangle$ as it transits between $|g_1\rangle$ and $|g_2\rangle$. We

then may apply the singular perturbation theory to remove the fast and stable dynamics of $|e\rangle$ in order to obtain a system living on the 2-level subspace span$\{|g_1\rangle, |g_2\rangle\}$.

The reduced Markovian master equation is still of Lindblad type and reads (see [10] for a detailed proof)

$$\frac{d}{dt}\rho = -\frac{\imath}{\hbar}[H,\rho] + \frac{1}{2}\sum_{j=1}^{2}(2L_j\rho L_j^\dagger - L_j^\dagger L_j\rho - \rho L_j^\dagger L_j), \quad (7)$$

where the reduced slow-Hamiltonian H is given, up to a global phase change, by

$$\tfrac{H}{\hbar} = \tfrac{\Delta}{2}(|g_2\rangle\langle g_2| - |g_1\rangle\langle g_1|) = \tfrac{\Delta}{2}\sigma_z \quad (8)$$

and

$$L_j = \sqrt{\tilde{\gamma}_j}\,|g_j\rangle\langle b_{\widetilde{\Omega}}| \qquad \text{with} \qquad \tilde{\gamma}_j = 4\tfrac{|\widetilde{\Omega}_1|^2+|\widetilde{\Omega}_2|^2}{(\Gamma_1+\Gamma_2)^2}\Gamma_j. \quad (9)$$

State

$$|b_{\widetilde{\Omega}}\rangle = \tfrac{\widetilde{\Omega}_1}{\sqrt{|\widetilde{\Omega}_1|^2+|\widetilde{\Omega}_2|^2}}|g_1\rangle + \tfrac{\widetilde{\Omega}_2}{\sqrt{|\widetilde{\Omega}_1|^2+|\widetilde{\Omega}_2|^2}}|g_2\rangle.$$

is known as the "bright state" in the physics literature (coherent population trapping). From now on, we deal with the 2-level system (7) instead of (6).

Master equation (7) is identical to the ensemble dynamics generated by the following single system Monte-Carlo trajectories. In the absence of quantum jumps, the system evolves through the dynamics (where $\{a,b\} = ab+ba$):

$$\tfrac{d}{dt}\rho = -\imath\frac{\Delta}{2}[\sigma_z,\rho] - \tfrac{1}{2}\sum_{j=1}^{2}\left\{L_j^\dagger L_j,\rho\right\} + \sum_{j=1}^{2}\mathrm{trace}(L_j^\dagger L_j\rho)\rho,$$

the Lindblad operators L_j being given by (9). Since $L_j^\dagger L_j = \tilde{\gamma}_j|b_{\widetilde{\Omega}}\rangle\langle b_{\widetilde{\Omega}}|$, we have, with $\tilde{\gamma} = \tilde{\gamma}_1+\tilde{\gamma}_2$,

$$\tfrac{1}{\tilde{\gamma}}\tfrac{d}{dt}\rho = -\imath\tfrac{\Delta}{2\tilde{\gamma}}[\sigma_z,\rho] - \tfrac{1}{2}\left\{|b_{\widetilde{\Omega}}\rangle\langle b_{\widetilde{\Omega}}|,\rho\right\} + \langle b_{\widetilde{\Omega}}|\rho|b_{\widetilde{\Omega}}\rangle\,\rho. \quad (10)$$

In addition, during each time step dt the system may jump towards the state $|g_j\rangle\langle g_j|$ with a probability given by

$$P_{\text{jump}}(\rho \to |g_j\rangle\langle g_j|) = \mathrm{trace}(L_j^\dagger L_j\rho)dt = \tilde{\gamma}_j\langle b_{\widetilde{\Omega}}|\rho|b_{\widetilde{\Omega}}\rangle\,dt, \quad j=1,2. \quad (11)$$

This probability is proportional to the population of the bright state $|b_{\widetilde{\Omega}}\rangle$ (which is actually the reason for its name).

B. Synchronization feedback

In this subsection, we consider the 2-level system obtained as the slow subsystem of the Λ-system presented in subsection III-A. Similarly to subsection II-B, we apply varying laser field amplitudes $\widetilde{\Omega}_1$ and $\widetilde{\Omega}_2$. Consider two positive constant Ω_1, Ω_2 and take the following modulations

$$\widetilde{\Omega}_1 = \Omega_1 + \imath\epsilon\Omega_2\cos(\omega t), \quad \widetilde{\Omega}_2 = \Omega_2 - \imath\epsilon\Omega_1\cos(\omega t) \quad (12)$$

with $\epsilon \ll 1$ and, to satisfy the assumptions of the above singular perturbations reduction, $\omega, \Omega_1, \Omega_2 \ll \Gamma_1, \Gamma_2$. By analogy with subsection III-A, consider the orthogonal basis

$$|b\rangle = \tfrac{\Omega_1|g_1\rangle+\Omega_2|g_2\rangle}{\sqrt{\Omega_1^2+\Omega_2^2}}, \quad |d\rangle = \tfrac{\Omega_2|g_1\rangle-\Omega_1|g_2\rangle}{\sqrt{\Omega_1^2+\Omega_2^2}} \quad (13)$$

which are respectively the "bright" and "dark" states of the nonoscillating system (i.e. with $\epsilon = 0$). Define

$$\gamma_j = 4\tfrac{\Omega_1^2+\Omega_2^2}{(\Gamma_1+\Gamma_2)^2}\Gamma_j \quad \text{for } j=1,2 \quad \text{and } \gamma = \gamma_1+\gamma_2.$$

Replacing Δ/γ by Δ, ω/γ by ω, and γt by t in (10),(11), we get quantum Monte-Carlo dynamics in the $1/\gamma$ scale, the optical-pumping scale. It reads as follows (with some abuse of notation):

- continuous-time (14)

$$\tfrac{d}{dt}\rho = -\imath[\frac{\Delta}{2}\sigma_z,\rho] - \tfrac{1}{2}\{|b+\imath\epsilon\cos(\omega t)d\rangle\langle b+\imath\epsilon\cos(\omega t)d|,\rho\} + \langle b+\imath\epsilon\cos(\omega t)d|\rho|b+\imath\epsilon\cos(\omega t)d\rangle\,\rho$$

with $|b\rangle = \cos\alpha|g_1\rangle + \sin\alpha|g_2\rangle$
$|d\rangle = -\sin\alpha|g_1\rangle + \cos\alpha|g_2\rangle$
$\alpha \in \left[0,\frac{\pi}{2}\right]$ the argument of $\Omega_1+i\Omega_2$

- jump to $\rho = |g_j\rangle\langle g_j|$, $j=1,2$ during dt with probability $P_{\text{jump}}(\rho \to |g_j\rangle\langle g_j|) = \frac{\gamma_j}{\gamma}\langle b+\imath\epsilon\cos(\omega t)d|\rho|b+\imath\epsilon\cos(\omega t)d\rangle\,dt$.

Each quantum jump leads to the emission of a photon. The total photon detection probability simply reads

$$p_{\text{alljumps}} = \langle b+\imath\epsilon\cos(\omega t)d|\rho|b+\imath\epsilon\cos(\omega t)d\rangle\,dt. \quad (15)$$

We assume a broadband detection process, where the only information available is the *time* of jump. The *type* of jump (to $\rho = |g_1\rangle\langle g_1|$ or to $\rho = |g_2\rangle\langle g_2|$) is not available. This means that, unlike in the two-level reduction of Section II, we do not know in which state the system is after each jump.

Similarly to Section II, the goal is to synchronize the lasers with the system's transition frequencies. Since Δ_e drops out of the reduced equations, we will make Δ converge to zero; this means that we synchronize on the difference between ground state frequencies $\frac{E_{g2}-E_{g1}}{\hbar}$.

We propose the following synchronization algorithm, assuming that $\delta, \epsilon \ll 1 \ll \omega$ ($\ll \Gamma_1, \Gamma_2$):

$$\begin{cases} \Delta(N+1) = \Delta(N) - \delta\sin(2\alpha)\cos(\omega t_N) \\ \qquad\qquad \text{if} \quad |\Delta(N) - \delta\sin(2\alpha)\cos(\omega t_N)| \le C, \\ \Delta(N+1) = C \qquad \text{otherwise} \end{cases} \quad (16)$$

at times t_N of photon detection for which there has been no photon emission during a preceding "dead-time" interval $[t_N - T, t_N)$. As in Section II, we impose bound C on detuning. Unlike for the V-system, but more like the traditional 2-level system in [9], the "dead-time" constant T is just a technical parameter necessary for the proof of the theorem: numerical simulations illustrate that in practice one can simply take $T = 0$.

The formal convergence result is similar to Theorem 1 for the V-system: if we *assume the system reduction to be exact*, then given any small ϵ (now appearing in the controller as well), we can adjust the parameters ω large and δ small

enough such that the detuning Δ_N converges on average to an $O(\epsilon^2)$-neighborhood of 0 with a deviation of order $O(\epsilon)$.

Theorem 2: Consider the Monte-Carlo trajectories described by (14) with update (16). Assume $\epsilon \ll 1$, $\frac{1}{\omega} \sim \epsilon^2$, $\delta \sim \epsilon^3$ and initial detuning $C < 1/2$. Then there exists a dead-time T large enough so that

$$\limsup_{N\to\infty} \mathbb{E}(\Delta(N)^2) \leq O(\epsilon^2)\,.$$

C. Numerical simulations

Like in Section II, we simulate the above synchronization strategy on the main Λ-system, and not on the slow 2-level subsystem resulting from approximate system reduction. We take the parameters $C = 0.5$, $\Omega_1 = \Omega_2 = 1$ (i.e., $\alpha = \pi/4$), $\Gamma_1 = \Gamma_2 = 3.0$ (i.e., $\gamma_1 = \gamma_2 = 0.6667$), $\epsilon = 0.03$, $\gamma/\omega = 0.05$, and $\delta = 0.015$. Dead-time is left at $T = 0$, very unlike for the V-system. The simulations of Figure 5 illustrate 10 random Monte-Carlo trajectories of the system starting at $\Delta_0 = 0.5$ and $\rho_0 = |d\rangle\langle d|$, where $|d\rangle = \frac{1}{\sqrt{2}}(|g_1\rangle - |g_2\rangle)$. The first plot provides the number of photon detections (quantum jumps) while the second one gives the evolution of detuning $\Delta(N)$. As can be noted, the detuning converges to a small neighborhood of zero within at most 1000 detections.

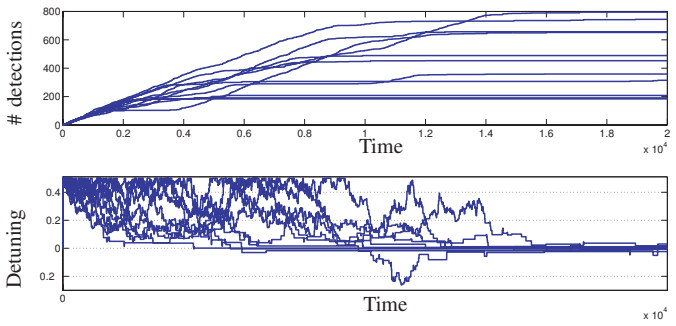

Fig. 5. Detuning evolution and number of quantum jumps (= photon detections) as a function of time for the synchronization feedback on the Λ-system.

IV. CONCLUSION

We have studied two atomic systems that are possible candidates for frequency standards: the first one consists of a so-called "V-configuration" with two excited states (one highly unstable and one metastable) and one stable ground state; the second one consists of a "Λ-configuration" with one highly unstable excited state and two metastable ground states. Both systems have been studied in the physics literature, the V-system widely as a candidate for an ultimate ultra-high-precision atomic clock and the Λ-system as a candidate for atomic microclocks. However, in such physics experiments, generally a cloud of atoms is considered as a statistical ensemble and the measured photocurrent is used to synchronize the laser fields.

In this paper, we propose a *real-time* output feedback method to lock the probe frequencies to the atomic ones in experiments where a *single* atom is probed and evolves according to inherently stochastic quantum dynamics. For both the V and Λ settings, we obtain theoretical real-time synchronization results after having reduced the system with singular perturbation theory. The synchronization results are further confirmed in full-model simulations. Precise synchronization capabilities allow to consider the case of a single-atom frequency standard, where a laser is tuned to an atom transition frequency that remains very accurately stable. Alternatively, the real-time tracking capability might be used to track variations of the energy levels in a single atom under influence of physical parameters (e.g. magnetic fields).

V. ACKNOWLEDGMENTS

The authors thank Guilhem Dubois from LKB and André Clairon from SYRTE for interesting discussions, suggestions and references in physics journals. This work was partially supported by the "Agence Nationale de la Recherche" (ANR), Projet Blanc CQUID number 06-3-13957 and Projet Jeunes Chercheurs EPOQ2 number ANR-09-JCJC-0070.

REFERENCES

[1] 13ème Conférence Générale des Poids et Mesures. Resolution 1. *Metrologia*, 4:41–45, 1968.
[2] E. Arimondo. Coherent population trapping in laser spectroscopy. *Progr. Optics*, 35:257–354, 1996.
[3] K.B. Ariyur and M. Krstic. *Real-time optimization by extremum-seeking control*. Wiley-Interscience, 2003.
[4] C. Cohen-Tannoudji and J. Dalibard. Single-atom laser spectroscopy. Looking for dark periods in fluorescence light. *Europhysics Letters*, 1(9):441–448, 1986.
[5] J. Dalibard, Y. Castin, and K. Mölmer. Wave-function approach to dissipative processes in quantum optics. *Phys.Rev.Lett.*, 68(5):580–583, 1992.
[6] R. Van Handel, J.K. Stockton, and H. Mabuchi. Feedback control of quantum state reduction. *IEEE Trans. Autom. Control*, 50:768–780, 2005.
[7] S. Haroche and J.-M. Raimond. *Exploring the Quantum: atoms, cavities and photons*. Oxford University Press, 2006.
[8] J. Kitching, S. Knappe, N. Vukicevic, L. Hollberg, R. Wynands, and W. Weidemann. A microwave frequency reference based on vcsel-driven dark line resonance in Cs vapor. *Trans. Instrum. Meas.*, 49:1313–1317, 2000.
[9] M. Mirrahimi and P. Rouchon. Real-time synchronization feedbacks for single-atom frequency standards. *SIAM J. Control Optim.*, 48(4):2820–2839, 2009.
[10] M. Mirrahimi and P. Rouchon. Singular perturbations and Lindblad-Kossakowski differential equations. *IEEE Trans. Automatic Control*, 54(6):1325–1329, 2009.
[11] W.H. Oskay, S.A. Diddams, E.A. Donley, T.M. Fortier, T.P. Heavner, L. Hollberg, W.M. Itano, S. R. Jefferts, M.J. Delaney, K. Kim, F. Levi, T.E. Parker, and J.C. Bergquist. Single-atom optical clock with high accuracy. *Phys. Rev. Lett.*, 97(2):020801.1–020801.4, 2006.
[12] E. Peik, T. Schneider, and Ch. Tamm. Laser frequency stabilization to a single ion. *J. Phys. At. Mol. Opt. Phys.*, 39:145–158, 2006.
[13] R.J. Rafac, B.C. Young, J.A. Beall, W.M. Itano, D.J. Wineland, and J.C. Bergquist. Sub-dekahertz ultraviolet spectroscopy of $^{199}Hg^+$. *Phys.Rev.Lett.*, 85(12):2462–2465, 2000.
[14] E. Riis and A.G. Sinclair. Optimum measurement strategies for trapped ion optical frequency standards. *J. Phys. At. Mol. Opt. Phys.*, 37:4719–4732, 2004.
[15] D.J. Wineland and H. Dehmelt. *Bull. Am. Phys. Soc.*, 20:637, 1975.